EXPERIMENTAL and MOLECULAR MEDICINE, Vol. 38, No. 2, 180-189, April 2006

# Implication of phosphorylation of the myosin II regulatory light chain in insulin-stimulated GLUT4 translocation in 3T3-F442A adipocytes

**Young Ok Choi[1], Hee Jeong Ryu[1], Hye Rim Kim[1], Young Sook Song[1], Cheonghwan Kim[1], Wan Lee[2], Han Choe[1], Chae Hun Leem[1] and Yeon Jin Jang[1,3]**

[1]Department of Physiology
University of Ulsan College of Medicine
Seoul 138-736, Korea
[2]Department of Biochemistry
College of Medicine, Dongguk University
Gyeongju 780-714, Korea
[3]Corresponding author: Tel, 82-2-3010-4274;
Fax, 82-2-3010-8135; E-mail, yjjang@amc.seoul.kr

Accepted 3 April 2006

Abbreviations: BAPTA/AM, bis (*o*-aminophenoxy)ethane-N,N,N',N' tetraacetic acetoxymethyl ester; BDM, 2,3-butanedione monoxime; HSP, high-speed pellet fraction; $[Ca^{2+}]_i$, intracellular $Ca^{2+}$ concentration; KRB, Krebs-Ringer bicarbonate buffer; MLCK, myosin light chain kinase; PM, plasma membrane fraction; RLC, regulatory light chain; 2-DG, 2-deoxyglucose

## Abstract

**In adipocytes, insulin stimulates glucose transport primarily by promoting the translocation of GLUT4 to the plasma membrane. Requirements for $Ca^{2+}$/calmodulin during insulin-stimulated GLUT4 translocation have been demonstrated; however, the mechanism of action of $Ca^{2+}$ in this process is unknown. Recently, myosin II, whose function in non-muscle cells is primarily regulated by phosphorylation of its regulatory light chain by the $Ca^{2+}$/calmodulin-dependent myosin light chain kinase (MLCK), was implicated in insulin-stimulated GLUT4 translocation. The present studies in 3T3-F442A adipocytes demonstrate the novel finding that insulin significantly increases phosphorylation of the myosin II RLC in a $Ca^{2+}$-dependent manner. In addition, ML-7, a selective inhibitor of MLCK, as well as inhibitors of myosin II, such as blebbistatin and 2,3-butanedione monoxime, block insulin- stimulated GLUT4 translocation and subsequent glucose transport. Our studies suggest that MLCK may be a regulatory target of $Ca^{2+}$/calmodulin and may play an important role in insulin-stimulated glucose transport in adipocytes.**

**Keywords:** calcium signaling; glucose transporter type 4; insulin; myosin type II; myosin-light-chain kinase; phosphorylation

## Introduction

Insulin stimulates glucose transport in adipocytes and skeletal muscle cells via regulated vesicular transport (reviewed in Watson *et al.*, 2004). In the absence of insulin, more than 95% of the insulin-sensitive glucose transporter, GLUT4, is sequestered in membranes of intracellular vesicles. Insulin activates various signaling pathways, which in turn provoke translocation and fusion of GLUT4-containing vesicles to the plasma membrane. This GLUT4 recruitment to the plasma membrane is mediated by SNARE (soluble *N*-ethylmaleimide-sensitive factor attachment protein receptor) proteins, such as vesicle-associated membrane protein 2, syntaxin 4, and synaptosome-associated 23-kDa protein.

In view of the role of $Ca^{2+}$ as an important second messenger in regulated exocytosis, numerous studies have examined the involvement of $Ca^{2+}$ in insulin-stimulated glucose transport. After extended controversy on this issue, it was recently shown that depletion of intracellular $Ca^{2+}$ with a membrane-permeable $Ca^{2+}$ chelator, bis (*o*-aminophenoxy)ethane-N,N,N',N' tetraacetic acetoxymethyl ester (BAPTA/AM), inhibits insulin-stimulated glucose transport in adipocytes (Chang *et al.*, 1999; Whitehead *et al.*, 2001; Worrall and Olefsky, 2002). A recent study showed that insulin increased $Ca^{2+}$ concentrations near the membrane even though it did not increase global cytoplasmic $Ca^{2+}$ concentrations in isolated skeletal muscle cells (Bruton *et al.*, 1999). In addition, inhibitors of calmodulin, a ubiquitous calcium-dependent regulatory protein, interfere with the effect of insulin on glucose transport (Shechter, 1984; Whitehead *et al.*, 2001). However, the mechanism(s) by which $Ca^{2+}$/calmodulin mediate the insulin-stimulated exocytosis of GLUT4-containing vesicles remains to be elucidated.

One of the mechanisms of action of $Ca^{2+}$ during

exocytosis might be the regulation of the interaction of cytoskeletal actin with myosin II. This interaction controls both actin dynamics and the interactions between vesicles and the cytoskeleton. Myosin II proteins, also called conventional myosins, consist of two heavy chains (i.e., 170-240 kDa) and two pairs of light chains (i.e., 16-23 kDa), named the RLC and the essential light chains (Sellers, 2000). In nonmuscle cells, the function of myosin II (including its interaction with actin) is primarily regulated by phosphorylation of its RLC, which is usually mediated by the $Ca^{2+}$/calmodulin-dependent enzyme, MLCK. There is considerable evidence for the necessity of RLC phosphorylation by MLCK, as well as for dynamic actomyosin interactions, in regulated exocytosis (Funaba *et al.*, 2003; Chou *et al.*, 2004; Neco *et al.*, 2004). In the case of adipocyte GLUT4, it is now well established that its optimal redistribution in response to insulin requires a dynamic actin rearrangement (i.e., polymerization/depolymerization) (Omata *et al.*, 2000; Kanzaki and Pessin, 2001; Jiang *et al.*, 2002). Interestingly, a recent study in 3T3-L1 adipocytes showed that myosin II activity, in association with actin, participated in insulin-stimulated glucose uptake (Steimle *et al.*, 2005). Myosin II-mediated contraction of actin filaments may contribute to either the movement of GLUT4-containing vesicles from the interior of cells to the cell surface or to cortical actin restructuring that is required for vesicular fusion. In the present study, we examined the possibility that $Ca^{2+}$/calmodulin-dependent phosphorylation of the RLC by MLCK may be involved in insulin-stimulated GLUT4 translocation in 3T3-F442A adipocytes.

## Materials and Methods

### Materials

Blebbistatin was purchased from Calbiochem (San Diego, CA), ML-7 was from Biomol (Plymouth Meeting, PA), BAPTA/AM and its 5,5'-dimethyl derivative (dimethyl-BAPTA/AM) were from TEFLAB (Austin, TX), trifluoperazine was from Smith Kline & French Laboratories (Philadelphia, PA), Sulfo-NHS-LC-biotin and streptavidin-agarose beads were from Pierce Biotechnology (Rockford, IL), 2-deoxy-D-[1-$^3$H]glucose (2-[$^3$H]DG) was from Amersham Corporation (Arlington Heights, IL), [$^{32}$P]orthophosphate was from Dupont/NEN (Boston, MA), BCS and FCS were from Hyclone (Logan, UT), DMEM and antibiotics were from GIBCO (Grand Island, NY), and insulin, phloretin, cytochalasin B, BDM, monoclonal Ab against a 20-kDa RLC subunit of myosin II, and other standard chemicals were from Sigma Chemical Company (St. Louis, MO). Polyclonal anti-GLUT1 Ab was obtained from Santa Cruz Biotechnology (Santa Cruz, CA). A polyclonal, affinity-purified, rabbit Ab against the C-terminus of GLUT4 was prepared as previously described (Jhun *et al.*, 1992).

### Cell culture

3T3-F442A murine fibroblasts (provided by Dr. H. Green at Harvard Medical School, Boston, MA) were maintained in DMEM supplemented with 10% BCS. This cell line is known to differentiate spontaneously (i.e., without insulin and dexamethasone supplementation) into adipocytes (Kuri-Harcuch and Green, 1978; Hainque *et al.*, 1990). Thus, differentiation was induced 24-48 h after confluence by altering the medium to DMEM supplemented with 10% FCS. The cells were used for experiments 10-12 days after induction of differentiation, when 90-95% of the cells had differentiated into adipocytes; differentiation was verified by intracytoplasmic lipid staining with Oil red O. This cell line was used in experiments until the 13th passage after isolation of clones.

### 2-Deoxyglucose (2-DG) uptake

3T3-F442A adipocytes in 24-well culture plates were incubated overnight in serum-free DMEM, washed, and then incubated in Krebs-Ringer bicarbonate buffer (KRB: 118 mM NaCl, 4.7 mM KCl, 1.3 mM $CaCl_2$, 1.2 mM $MgSO_4$, 1.2 mM $NaH_2PO_4$, and 25 mM $NaHCO_3$, pH 7.4) containing 0.5 mM glucose and 2% BSA at 37$^o$C in humidified air containing 5% $CO_2$. In some experiments, "$Ca^{2+}$-free KRB", prepared by omitting $CaCl_2$ and adding 6 mM EGTA, was used to exclude extracellular $Ca^{2+}$. Insulin (100 nM) was added 30 min prior to measurement of 2-DG uptake and inhibitors were added 30 min prior to insulin at the final concentration indicated in the figure legends. Measurement of 2-DG uptake was initiated by the addition of 2-[$^3$H]DG at a final concentration of 0.2 mM (2.8 mCi/mmol) and was terminated after 3 min by the addition of 1.5 ml ice-cold KRB containing 0.2 mM phloretin. Cells were washed twice rapidly with ice-cold KRB, air-dried, and solubilized in 0.4 ml of a 0.1% SDS solution. Cellular radioactivity was measured by liquid scintillation counting. Nonspecific uptake was determined in parallel samples containing 0.4 mM phloretin and 0.04 mM cytochalasin B and this value was subtracted from each total uptake determination.

### Subcellular membrane fractionation and immunoblotting

Subcellular fractions were prepared as described by Clark *et al.* (1998) with minor modifications. After

rapid rinsing with ice-cold PBS, the cells were scraped into buffer A (20 mM Hepes, 1 mM EDTA, and 250 mM sucrose, pH 7.4) containing 1 mM PMSF and a protease inhibitor mix (Roche Applied Science, Germany) and disrupted by 10 passages through a 25-gauge needle as described by Nave *et al*. (1996). All subsequent preparations were done on ice or at 4°C. The homogenate was centrifuged at 3,000 *g* for 10 min to remove lipids and precipitated cellular debris. The remainder of the homogenate was centrifuged at 16,000 *g* for 20 min. The pellet was then resuspended in 1 ml of buffer A, layered onto a 3-ml sucrose cushion (1.2 M), and subjected to ultracentrifugation at 100,000 *g* for 70 min. The membrane fraction floating on the sucrose cushion was collected, resuspended in 10 ml of buffer A, and centrifuged at 48,000 *g* for 45 min. The final pellet, designated as the plasma membrane fraction (PM), was resuspended in HESN buffer (20 mM Hepes, 1 mM EDTA, 250 mM sucrose, and 100 mM NaCl, pH 7.4). The supernatant from the 16,000 *g* centrifugation was subjected to additional centrifugation at 30,000 *g* for 20 min. The supernatant from this separation was further centrifuged at 200,000 *g* for 90 min and the resulting pellet, designated as the high-speed pellet fraction (HSP; also referred to as the low density microsomal fraction), was also resuspended in HESN buffer. Protein concentrations were determined using the Bradford assay kit (Bio-Rad, Hercules, CA) with BSA as a standard.

Aliquots of proteins from these subcellular fractions were solubilized in Laemmli sample buffer. Gel elelctrophoresis and immunoblotting were performed as previously described (Park *et al.*, 2005). Proteins were separated by SDS-PAGE and transferred to a nitrocellulose membrane. Membranes were blocked with 5% skim milk in TBST buffer (10 mM Tris, 150 mM NaCl, and 0.05% Tween 20, pH 7.4) for 1 h at room temperature. The membranes were incubated overnight at 4°C with either anti-GLUT1 or anti-GLUT4 Abs. After incubation, the membranes were then washed with TBST buffer and incubated for 1 h at room temperature with horseradish peroxidase-conjugated secondary Abs. The proteins were then detected using ECL reagent, and the resulting signals were quantified using a video densitometer (Model 620, Bio-Rad) in the reflective mode.

### Cell surface biotinylation

Cell surface biotinylation was performed according to a previously published procedure (Dransfeld *et al.*, 2000). The cells were washed with ice-cold PBS and incubated with 1 ml of 0.5 mg/ml Sulfo-NHS-LC-biotin in PBS for 30 min at 4°C. The reaction was stopped by rinsing the cells with 15 mM glycine in ice-cold PBS. The cells were then collected and solubilized for 30 min at 4°C in 1 ml solubilization buffer (165 mM NaCl, 20 mM Hepes, 1% Triton X-100, 1 mM EGTA, and a protease inhibitor mix, pH 7.4). The lysate was centifuged at 16,000 *g* for 20 min. The supernatant was gently mixed overnight with 50 μl streptavidin-agarose beads at 4°C and then centrifuged at 2,500 *g* for 1 min. The bead pellet was washed three times with 1 ml ice-cold wash buffer (150 mM NaCl, 10 mM Tris, and a protease inhibitor mix, pH 7.0). The final pellet was resuspended in 120 μl (1.2×) Laemmli sample buffer and incubated for 30 min at 65°C. The supernatant that was separated from the beads by centrifugation was collected. The samples were subjected to immunoblot analysis using anti-GLUT4 Ab.

### Determination of RLC phosphorylation

Phosphorylation of the RLC was estimated according to the method proposed by Hainque *et al*. (Hainque *et al.*, 1990). Cells were incubated overnight with serum- and $PO_4$-free DMEM, and then labeled metabolically with 200 μCi/ml [$^{32}$P]orthophosphate in $PO_4$-free DMEM for 4 h at 37°C. After washing with $PO_4$-free DMEM, the cells were incubated for 1 h in either DMEM or "$Ca^{2+}$-free DMEM" (i.e., composition was identical to DMEM except that $CaCl_2$ was omitted and 50 μM dimethyl-BAPTA/AM and 2 mM EDTA were added). The cells were then incubated for 30 min in the presence or absence of 100 nM insulin. Whole cell lysates were prepared as described below. The cells were disrupted on ice in 200 μl lysis buffer (1% NP-40, 100 mM sodium pyrophosphate, 50 mM NaF, 5 mM EGTA, 0.1 mM PMSF, 10 μg/ml leupeptin, 10 mM β-mercaptoethanol, 20 mM Tris-HCl, and 1 mM sodium orthovanadate, pH 8.6). The cells were scraped, subjected to 3 cycles of freezing-thawing, and sonicated on ice. The lysates were centrifuged at 16,000 *g* at 4°C for 30 min and the supernatants were collected. These cell lysates were subjected to immunoblot analysis using a monoclonal anti-RLC Ab. Autoradiography of phosphorylated RLC was performed using Kodak X-OMT AR film at -70°C with an intensifying screen (Hypercassette, Amersham). The extent of RLC phosphorylation was quantified as the ratio of band densities on the autoradiogram to those on the immunoblot membrane.

### Statistical analysis

The observed values are presented as mean ± SE. Student's paired or unpaired *t*-tests were performed as indicated for pair-wise group comparisons, and analysis of variance, followed by the Bonferroni test, was used when more than two groups were com-

pared. Differences were considered significant at $P < 0.05$.

## Results and Discussion

In 3T3-F442A adipocytes, 2-DG uptake rate was 24 ± 1.6 pmol/well/min in the basal state and increased approximately 5 fold after 100 nM insulin treatment ($n = 8$; $P < 0.01$; Figure 1A). Immunoblot analysis of the subcellular membrane fractions showed that at least two distinct glucose transporters, GLUT4 and GLUT1, were present in these spontaneously differentiated 3T3-F442A adipocytes. Consistent with previous reports, 100 nM insulin increased GLUT4 levels in the PM by 4.2 fold and correspondingly decreased GLUT4 levels in the HSP (Figure 1B). Unlike GLUT4, GLUT1 was primarily, if not entirely, located in the PM; its level in the PM was unaltered by insulin (Figure 1C). Thus, it is apparent in these 3T3-F442A adipocytes that an enhancement of glucose transport by insulin is mainly, if not completely, due to increased GLUT4 levels in the plasma membrane.

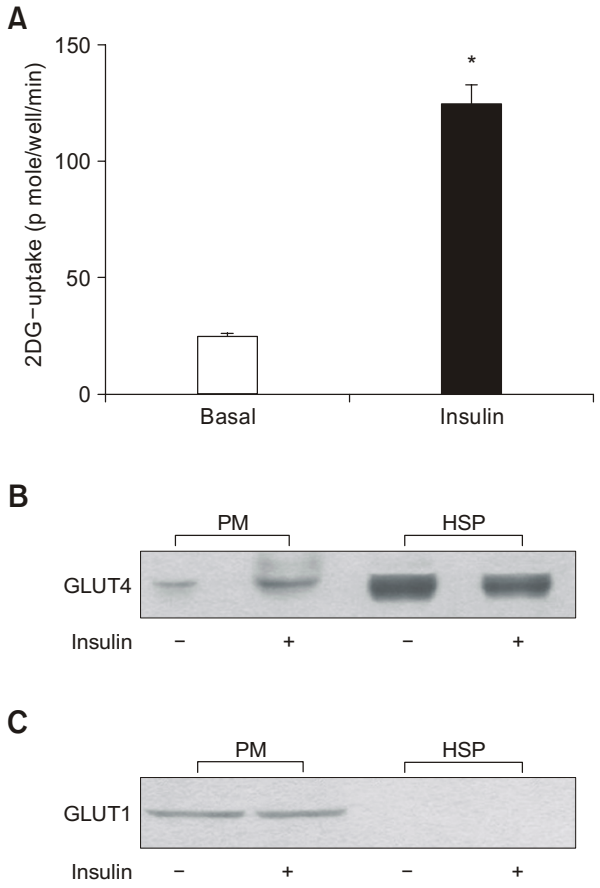


**Figure 1.** Effects of insulin on 2-DG uptake (A) and intracellular distribution of GLUT4 (B) and GLUT1 (C) in spontaneously differentiated 3T3-F442A adipocytes. (A) Cells were incubated with or without (basal) 100 nM insulin for 30 min and then subjected to measurements of rates of 2-DG uptake ($n = 8$). *$P < 0.01$ *vs.* basal only. (B & C) After incubation, cell lysates were fractionated into plasma membrane (PM) and high speed pellet (HSP) fractions. The blots are representative of 2 independent experiments.

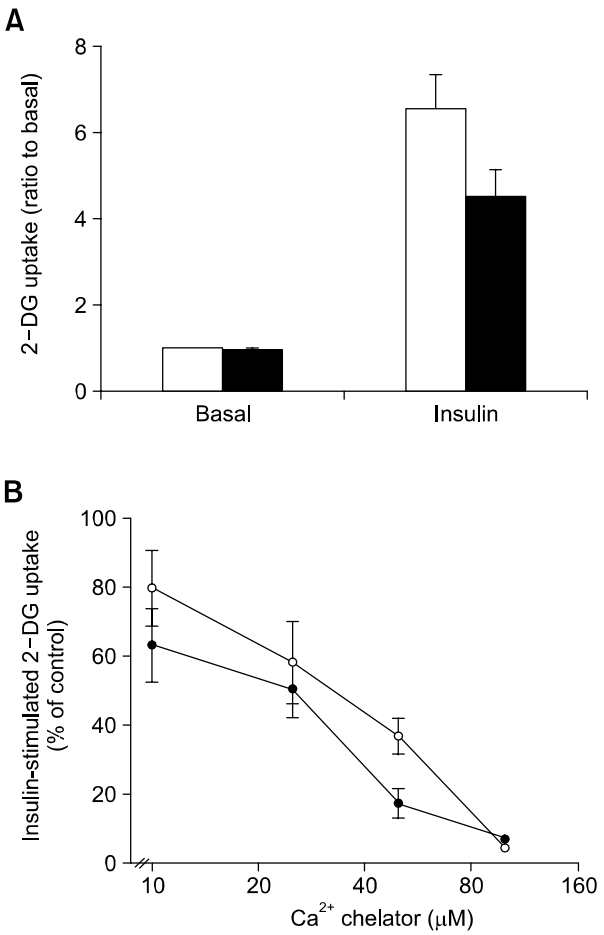


**Figure 2.** Role of $Ca^{2+}$ in insulin-stimulated glucose transport. (A) Effect of exclusion of $Ca^{2+}$ from the extracellular buffer. Cells were incubated in either normal KRB (open bar) or KRB lacking $CaCl_2$ but containing 6 mM EGTA (closed bar) and subjected to measurements of basal and insulin-stimulated 2-DG uptake ($n = 4$). (B) Dose-response curves of BAPTA/AM (open circles) and dimethyl-BAPTA/AM (closed circles) during insulin-stimulated 2-DG uptake. Cells were preincubated with or without an intracellular $Ca^{2+}$ chelator for 30 min and were then incubated with or without (basal) 100 nM insulin for an additional 30 min prior to the determination of the rate of 2-DG uptake. The results are expressed as the percentage of cellular insulin-stimulated 2-DG uptake above basal without pretreatment (control). Data represent an average of 3 experiments and each was measured in triplicate.

### $Ca^{2+}$/calmodulin are required for insulin-stimulated GLTU4 translocation

We next examined the involvement of $Ca^{2+}$ in insulin-stimulated glucose transport in 3T3-F442A adipocytes. In agreement with a previous study in 3T3-L1 cells (Whitehead *et al.*, 2001), excluding extracellular $Ca^{2+}$ by incubating the cells in $Ca^{2+}$-free buffer reduced insulin-stimulated 2-DG uptake by 30% (Figure 2A). To further investigate the relationship between the intracellular $Ca^{2+}$ concentration ($[Ca^{2+}]_i$) and the effect of insulin on glucose transport, we preincubated cells with two membrane-permeable $Ca^{2+}$ chelators that have different affinities for $Ca^{2+}$, BAPTA/AM ($k_d$ = 130 nM) and dimethyl-BAPTA/AM ($k_d$ = 40 nM) (Tsien, 1980). BAPTA/AM (10-100 μM) inhibited insulin-stimulated 2-DG uptake in a dose-dependent manner (open circles in Figure 2B), as previously reported (Chang *et al.*, 1999; Whitehead *et al.*, 2001; Worrall and Olefsky, 2002). Its dimethyl derivative, with a higher affinity for $Ca^{2+}$, blocked the insulin effect more efficiently, as represented by the leftward shift of the dose-response curve (closed circles in Figure 2B). These data, shown in Figure 2A and B, suggest a functional correlation between $[Ca^{2+}]_i$ and insulin-stimulated glucose transport even though direct measurements of $[Ca^{2+}]_i$ were not made.

In Figure 3, the effect of dimethyl-BAPTA/AM on insulin-stimulated GLUT4 translocation was examined using immunodetection of GLUT4 in cell surface-biotinylated protein-fractions. Insulin raised the level of GLUT4 at the cell surface by 4.9 ± 0.4 fold ($n$ = 3); pretreatment with 50 μM dimethyl-BAPTA/AM inhibited this insulin effect by approximately 80% (Figure 3), similar to the inhibition of 2-DG uptake (closed circle in Figure 2B). These results suggest a key role for $Ca^{2+}$ in the mediation of the effects of insulin on GLUT4 translocation. Taking into consideration of the well-documented requirement for $Ca^{2+}$ in both synaptic vesicle fusion and vesicle fusion/exocytosis in nonneuronal cells, $Ca^{2+}$ is expected to play a role in the insulin-stimulated trafficking and/or fusion processes of GLUT4 vesicles.

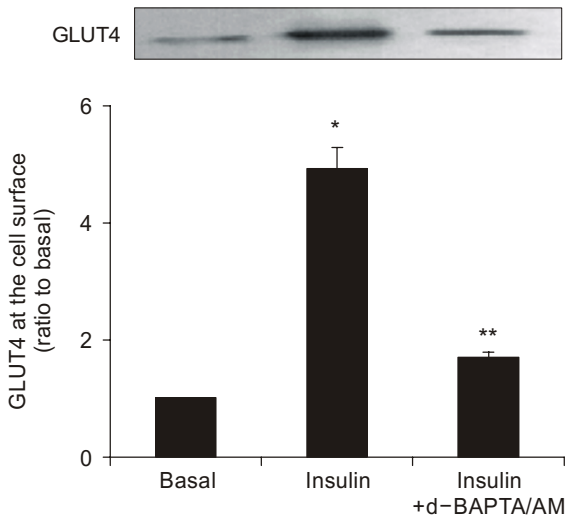


**Figure 3.** Effects of dimethyl-BAPTA/AM on insulin-stimulated GLUT4 translocation. Cells were preincubated with or without 50 μM dimethyl-BAPTA/AM for 30 min and were then incubated in the presence or absence of 100 nM insulin for another 30 min. The level of GLUT4 on the cell surface was determined by cell surface biotinylation as described in the Methods. Representative blots from 3 separate experiments are presented. The bar graph represents the result from densitometric analysis of the blots. *$P < 0.05$ *vs.* basal; **$P < 0.05$ *vs.* insulin only.

It is also possible that $Ca^{2+}$ may be involved in insulin-stimulated signal transduction pathways. It was previously observed that BAPTA/AM inhibited insulin-stimulated Akt phosphorylation (Whitehead *et al.*, 2001; Worrall and Olefsky, 2002). However, a quantitative analysis of the dose-response curves of both Akt phosphorylation and glucose transport indicate that inhibition of Akt phosphorylation may not be the primary mechanism by which BAPTA/AM reduces insulin-stimulated glucose transport (Whitehead *et al.*, 2001; Worrall and Olefsky, 2002).

The role of $Ca^{2+}$ in insulin-stimulated glucose transport has remained unresolved despite extensive investigation. This is mainly because of the controversial results from experiments with $Ca^{2+}$ depletion and the failure to detect an increase in $[Ca^{2+}]_i$ upon insulin stimulation. However, our results (Figure 2 and 3), together with results from other studies using BAPTA/AM (Chang *et al.*, 1999; Whitehead *et al.*, 2001; Worrall and Olefsky, 2002), clearly demonstrate that $Ca^{2+}$ is required for insulin-stimulated glucose transport in adipocytes. Thus, negative evidence for the requirement of $Ca^{2+}$ in the previous studies using other methods of $Ca^{2+}$ depletion (Cheung *et al.*, 1987; Klip and Ramlal, 1987), seems to be attributed to an incomplete control of $[Ca^{2+}]_i$ upon cellular stimulation by insulin (as discussed in Whitehead *et al.*, 2001). In addition, Bruton *et al*. (1999), using a modified $Ca^{2+}$ indicator with a fat-soluble tail, demonstrated that insulin causes a significant increase in $Ca^{2+}$ levels near the plasma membrane but not in global cytoplasmic $Ca^{2+}$ concentrations. Such a localized increase would not be demonstrable by conventional $Ca^{2+}$ measurement techniques and provides a likely explanation for the failure to detect changes in $[Ca^{2+}]_i$ in previous studies; such an increase would still be subject to inhibition, however, with either BAPTA/AM or dimethyl-BAPTA/AM treatment.

During insulin-stimulated glucose transport, $Ca^{2+}$ appears to exert its effects via calmodulin-dependent

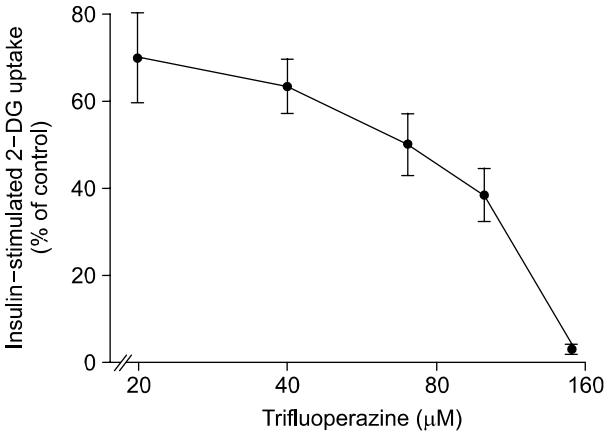


**Figure 4.** Dose-response curves of trifluoperazine, a calmodulin antagonist, during insulin-stimulated 2-DG uptake. Cells were preincubated with or without an trifluoperazine for 30 min and were then incubated with or without (basal) 100 nM insulin for an additional 30 min prior to the determination of the rate of 2-DG uptake. The results are expressed as the percentage of cellular insulin-stimulated 2-DG uptake above basal without pretreatment (control). Thus, insulin effect in the control condition without pretreatment of the drug is set at 100%. Data represent an average of 4 experiments and each was measured in triplicate.

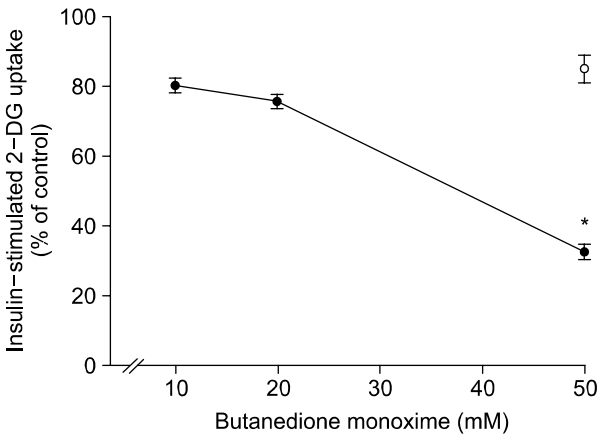


**Figure 5.** Effects of 2,3-butanedione monoxime (BDM), an inhibitor of myosin ATPase. Cells were preincubated with or without BDM (10-50 mM) or 50 mM sucrose for 30 min prior to the addition of vehicle (basal) or 100 nM insulin. The results are expressed as the percentage of cellular insulin-stimulated 2-DG uptake above basal without pretreatment (control). Data represent an average of 8 experiments and each was measured in triplicate. *$P < 0.05$ *vs.* 50 mM sucrose.

processes as calmodulin inhibitors have been shown to block such effects of insulin (Shechter, 1984; Yang *et al.*, 2000; Whitehead *et al.*, 2001). Consistent with these observations, calmodulin antagonists, such as trifluoperazine (Figure 4) and calmidazolium (data not shown), inhibited insulin-stimulated 2-DG uptake in a dose-dependent manner. Thus, our current results support the notion that $Ca^{2+}$/calmodulin are required for the insulin-stimulated recruitment of GLUT4 to the cell surface in adipocytes.

## MLCK is implicated in insulin-stimulated GLUT4 translocation

Calmodulin is a ubiquitous $Ca^{2+}$-dependent regulatory protein with multiple regulatory targets. One group of well-characterized regulatory targets is the calmodulin-regulated kinases including calmodulin-dependent protein kinase II and MLCK. In addition, insulin-stimulated GLUT4 translocation from the adipocyte interior to the plasma membrane requires the actin cytoskeleton. An actin-associated molecular motor, myosin II, has been suggested to participate in the mediation of this action of insulin (Lee *et al.*, 1997; Steimle *et al.*, 2005). Generally, in nonmuscle cells, actomyosin interactions are regulated by $Ca^{2+}$-dependent phosphorylation on specific sites in the RLC of the myosin II molecules by MLCK. In the context of these considerations, we believe that one of the $Ca^{2+}$/calmodulin-dependent kinases, MLCK, a dedicated protein kinase whose substrate specificity is restricted to the RLC of myosin II (Gallagher *et al.*, 1997), may be a regulatory target for adipocyte $Ca^{2+}$/calmodulin. It may also play an important role in stimulating glucose transport in response to insulin. In the present study, we have attempted to prove this hypothesis through a series of experiments.

First, we determined whether myosins are involved in insulin-stimulated glucose transport in 3T3-F442A adipocytes. Pretreatment of cells with BDM, an inhibitor of myosin ATPase (Herrmann *et al.*, 1992), significantly decreased insulin-mediated 2-DG uptake in a concentration-dependent manner ($n = 8$; $P < 0.01$; Figure 5). At a concentration of 50 mM, BDM reduced the insulin effect by 68 ± 3% ($n = 8$; $P < 0.01$ *vs.* insulin only), whereas 50 mM sucrose, which was expected to exert a similar osmotic effect as BDM, reduced the effect of insulin only by 15 ± 4% ($n = 8$; $P > 0.09$ *vs.* insulin only). The myosin motor protein family consists of many distinct isoforms, several of which are inhibited by BDM. Next, we tried blebbistatin (100 μM), a highly specific inhibitor of nonmuscle myosin II, and observed a significant inhibition of insulin-stimulated 2-DG uptake ($n = 9$; $P < 0.01$; Figure 6A). In addition, blebbistatin inhibited insulin-stimulated GLUT4 translocation by 50%, as determined by cell surface biotinylation (Figure 6B), demonstrating a degree of inhibition comparable to that observed on 2-DG uptake. Recently, Steimle *et al*. (Steimle *et al.*, 2005) demonstrated the lack of a blebbistatin effect on insulin-stimulated Akt phosphorylation despite significant inhibition of glucose transport in 3T3-L1 adi-

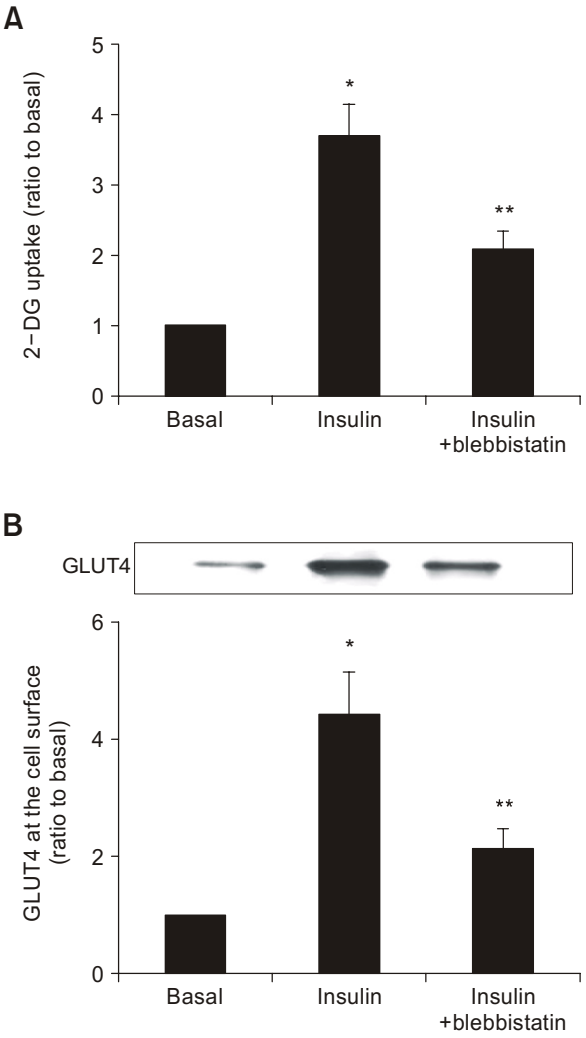


**Figure 6.** Effects of blebbistatin, a specific inhibitor of nonmuscle myosin II, on insulin-stimulated 2-DG uptake (A) and GLUT4 translocation (B). (A) Cells were preincubated with or without blebbistatin (100 μM) for 30 min and were then incubated with or without (basal) 100 nM insulin for an additional 30 min prior to the determination of the rate of 2-DG uptake. The results are expressed as the percentage of cellular insulin-stimulated 2-DG uptake above basal without pretreatment (control) ($n$ = 9). (B) The level of GLUT4 at the cell surface was determined by biotinylation of the following groups of cells: basal, insulin-stimulated (100 nM, 30 min), and insulin-stimulated with blebbistatin pretreatment (100 μM, 30 min). Representative blots from 3 separate experiments are presented. The bar graph represents the result from densitometric analysis of the blots. *$P < 0.05$ *vs.* basal; **$P < 0.05$ *vs.* insulin only.

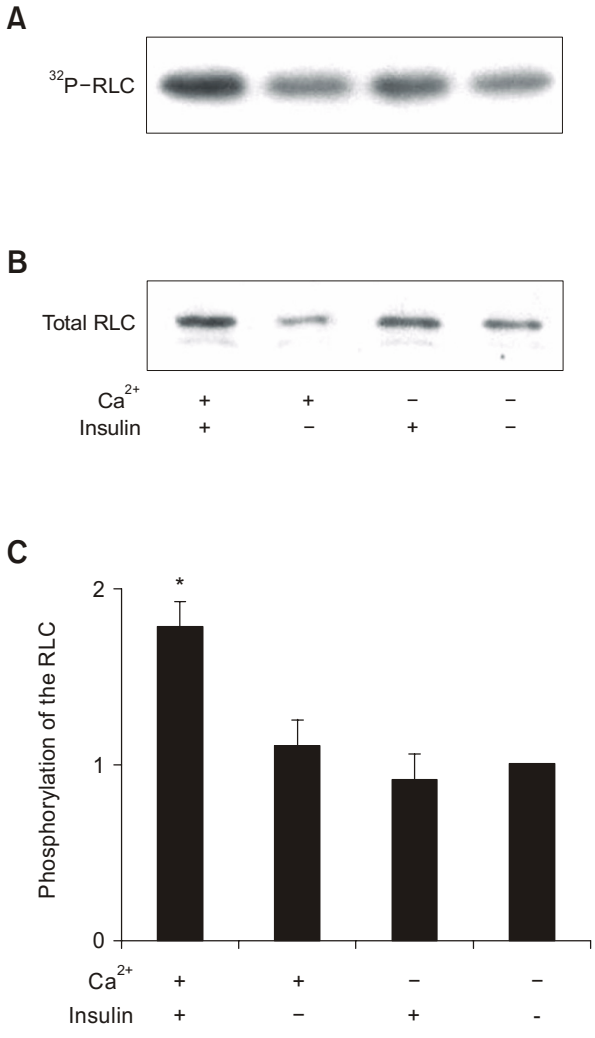


**Figure 7.** Insulin induces phosphorylation of the myosin II RLC in the presence of $Ca^{2+}$. Cells were incubated with 200 μ*Ci*/ml [$^{32}$P]orthophosphate in $PO_4$-free DMEM for 4 h ($n$ = 4 for each). After incubation for 1 h in either DMEM or "$Ca^{2+}$-free DMEM" as described in the Methods, the cells were incubated for 30 min in the presence or absence of 100 nM insulin and then lysed. Cell lysates were resolved by SDS-PAGE. (A) Autoradiography of phosphorylated RLC was performed using Kodak X-OMT AR film at -70°C with an intensifying screen. (B) The RLC was identified by immunoblot analysis using a monoclonal anti-RLC Ab. The blots in A and B are representative blots from 4 independent experiments with similar results. (C) The extent of RLC phosphorylation was quantified as the ratio of band densities on the autoradiogram to those on the immunoblot. The results are expressed as the change in the ratio relative to that of lane 4, which for comparative purposes, is set at 1.0. *$P < 0.05$ *vs.* lane 4.

pocytes. Collectively, our results imply that the activity of myosin II is required for insulin action on glucose transport in adipocytes, even though a possible involvement of other myosin isoforms, such as Myo1c (Bose *et al.*, 2002), cannot be excluded. Therefore, in the present study, we have focused on the potential role of myosin II activity in insulin-stimulated GLUT4 translocation.

In the case of nonmuscle myosin II, its ATPase activity is activated by actin after Ser-19 of the RLC is phosphorylated, usually by MLCK (Bresnick, 1999). Thus, we next examined the effects of insulin on RLC phosphorylation (Figure 7). Intriguingly, insulin treatment significantly increased the extent of

RLC phosphorylation by 70% (lane 1 *vs.* lane 2; $n$ = 4; $P < 0.02$) when cells were incubated in normal KRB containing 1.3 mM $Ca^{2+}$. This insulin effect was completely blocked by depleting intracellular $Ca^{2+}$ using dimethyl-BAPTA/AM (lane 3 *vs.* lane 1; $n$ = 4; $P < 0.01$). In the absence of insulin, RLC phosphorylation was unaffected by the availability of $Ca^{2+}$ (lane 2 *vs.* lane 4; $n$ = 4; $P > 0.9$). These novel observations clearly demonstrate that insulin increases the $Ca^{2+}$-dependent phosphorylation of the myosin II RLC.

Taken together, insulin stimulates both RLC phosphorylation (Figure 7) as well as GLUT4 translocation (Figure 1B and 3); depletion of $Ca^{2+}$ blocks both effects of insulin (Figures 3 and 7). This correlation suggests that phosphorylation of the RLC by MLCK may mediate the insulin signal to stimulate the translocation of GLUT4 downstream of $Ca^{2+}$/calmodulin. This idea is consistent with recent studies demonstrating that RLC phosphorylation plays a key role in the regulation of the exocytosis of secretory vesicles from chromaffin cells (Neco *et al.*, 2004) and of aquaporin 2 in the collecting ducts of the kidney (Chou *et al.*, 2004). However, increased phosphorylation of the RLC, shown in Figure 7, does not provide direct evidence for the participation of MLCK in insulin action since the RLC contains many protein kinase phosphorylation sites (Bresnick, 1999).

We employed ML-7, a synthetic naphthalene sulphonyl derivative of diazepine that selectively inhibits MLCK (Saitoh *et al.*, 1987), to test whether MLCK is involved in insulin-stimulated glucose transport (Figure 8). Pretreatment of cells with ML-7 (100 μM) for 30 min significantly inhibited insulin-stimulated 2-DG uptake (Figure 8A) as well as GLUT4 translocation (Figure 8B). The effects of ML-7 on GLUT4 translocation were somewhat greater than the effects on 2-DG uptake: it completely blocked the insulin-stimulated increase in GLUT4 levels at the cell surface ($n$ = 3; $P < 0.05$) but inhibited only about 50% of 2-DG uptake ($n$ = 5; $P < 0.01$). At present, there is no clear explanation for this discrepancy between the effects of ML-7 on 2-DG uptake and GLUT4 translocation, and hence, more detailed experiments are required. Nonetheless, it is obvious that the MLCK inhibitor, ML-7, inhibits insulin-stimulated GLUT4 translocation, implicating MLCK in the mechanism of action of insulin on glucose transport. In further support of this hypothesis, it was observed in our preliminary studies that suppression of MLCK expression via stably expressing antisense-MLCK decreased insulin-stimulated 2-DG uptake in 3T3-L1 adipocytes (unpublished data).

In conclusion, we provide evidence that $Ca^{2+}$/calmodulin are required for insulin-stimulated glucose transport in 3T3-F442A adipocytes. Our studies present a novel finding that insulin phosphorylates the RLC of myosin II in a $Ca^{2+}$-dependent manner. Consistent with a previous report (Steimle *et al.*, 2005), inhibitors of myosin II block insulin-stimulated glucose transport, suggesting a role for myosin II in GLUT4 translocation. Moreover, the

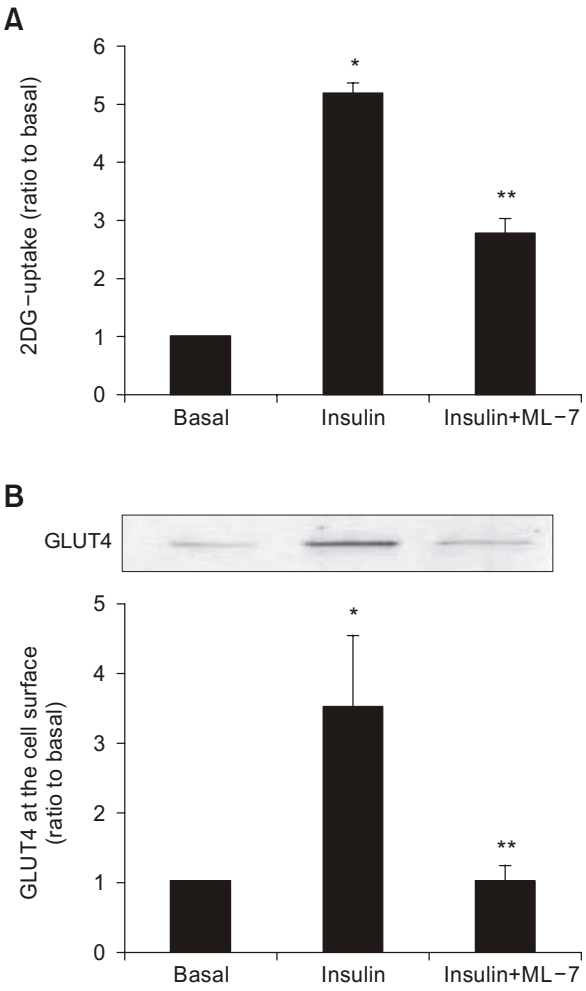


**Figure 8.** Effect of ML-7, a selective inhibitor of MLCK, on insulin-stimulated 2-DG uptake (A) and GLUT4 translocation (B). (A) Cells were preincubated with or without ML-7 (100 μM) for 30 min and were then incubated with or without (basal) 100 nM insulin for an additional 30 min prior to the determination of the rate of 2-DG uptake. The results are expressed as the percentage of cellular insulin-stimulated 2-DG uptake above basal without pretreatment (control). Data represent an average of 5 experiments and each was measured in triplicate. (B) The level of GLUT4 at the cell surface was determined by biotinylation of the following groups of cells: basal, insulin-stimulated (100 nM, 30 min), and insulin-stimulated with ML-7 pretreatment (100 μM, 30 min). Representative blots from 3 separate experiments are presented. The bar graph represents the result from densitometric analysis of the blots. *$P < 0.05$ *vs.* basal; **$P < 0.05$ *vs.* insulin only.

$Ca^{2+}$/calmodulin-dependent MLCK may play a key role in GLUT4 translocation since inhibition of MLCK by the selective inhibitor ML-7 abrogates insulin-stimulated GLUT4 translocation to the plasma membrane. Further studies are therefore needed to determine the precise role of MLCK in insulin-stimulated glucose transport.

**Acknowledgement**

This study was supported in part by grant no. R04-2002-000-00133-0 from the Basic Research Program of the Korean Science & Engineering Foundation and in part by grant no. 01-285 from the Asan Institute for Life Sciences, Seoul, Republic of Korea. The authors gratefully acknowledge Dr. Chun Sik Park for helpful discussion. The current address of C. Kim is Department of Orthopedic Surgery, Gang Neung Asan Hospital, Gang Neung, Republic of Korea.

## References

Bose A, Guilherme A, Robida SI, Nicoloro SM, Zhou QL, Jiang ZY, Pomerleau DP, Czech MP. Glucose transporter recycling in response to insulin is facilitated by myosin Myo1c. Nature 2002;420:821-4

Bresnick AR. Molecular mechanisms of nonmuscle myosin-II regulation. Curr Opin Cell Biol 1999;11:26-33

Bruton JD, Katz A, Westerblad H. Insulin increases near-membrane but not global $Ca^{2+}$ in isolated skeletal muscle. Proc Natl Acad Sci USA 1999;96:3281-6

Chang S, Jang YJ, Park K, Kim GS, Ryu HJ, Park CS. Role of $Ca^{2+}$ in the stimulation of glucose transport by insulin in adipocytes. Korean J Physiol Pharmacol 1999;3:357-64

Cheung JY, Constantine JM, Bonventre JV. Cytosolic free calcium concentration and glucose transport in isolated cardiac myocytes. Am J Physiol 1987;252:C163-72

Chou CL, Christensen BM, Frische S, Vorum H, Desai RA, Hoffert JD, de Lanerolle P, Nielsen S, Knepper MA. Non-muscle myosin II and myosin light chain kinase are downstream targets for vasopressin signaling in the renal collecting duct. J Biol Chem 2004;279:49026-35

Clark SF, Martin S, Carozzi AJ, Hill MM, James DE. Intracellular localization of phosphatidylinositide 3-kinase and insulin receptor substrate-1 in adipocytes: potential involvement of a membrane skeleton. J Cell Biol 1998;140:1211-25

Dransfeld O, Uphues I, Sasson S, Schurmann A, Joost HG, Eckel J. Regulation of subcellular distribution of GLUT4 in cardiomyocytes: Rab4A reduces basal glucose transport and augments insulin responsiveness. Exp Clin Endocrinol Diabetes 2000;108:26-36

Funaba M, Ikeda T, Abe M. Degranulation in RBL-2H3 cells: regulation by calmodulin pathway. Cell Biol Int 2003;27: 879-85

Gallagher PJ, Herring BP, Stull JT. Myosin light chain kinases. J Muscle Res Cell Motil 1997;18:1-16

Hainque B, Guerre-Millo M, Hainault I, Moustaid N, Ward-zala LJ, Lavau M. Long term regulation of glucose transporters by insulin in mature 3T3-F442A adipose cells. Differential effects on two glucose transporter subtypes. J Biol Chem 1990;265:7982-6

Herrmann C, Wray J, Travers F, Barman T. Effect of 2,3-butanedione monoxime on myosin and myofibrillar ATPases. An example of an uncompetitive inhibitor. Biochemistry 1992;31:12227-32

Jhun BH, Rampal AL, Liu H, Lachaal M, Jung CY. Effects of insulin on steady state kinetics of GLUT4 subcellular distribution in rat adipocytes. Evidence of constitutive GLUT4 recycling. J Biol Chem 1992;267:17710-5

Jiang ZY, Chawla A, Bose A, Way M, Czech MP. A phosphatidylinositol 3-kinase-independent insulin signaling pathway to N-WASP/Arp2/3/F-actin required for GLUT4 glucose transporter recycling. J Biol Chem 2002;277:509-15

Kanzaki M, Pessin JE. Insulin-stimulated GLUT4 translocation in adipocytes is dependent upon cortical actin remodeling. J Biol Chem 2001;276:42436-44

Klip A, Ramlal T. Cytoplasmic $Ca^{2+}$ during differentiation of 3T3-L1 adipocytes. Effect of insulin and relation to glucose transport. J Biol Chem 1987;262:9141-6

Kuri-Harcuch W, Green H. Adipose conversion of 3T3 cells depends on a serum factor. Proc Natl Acad Sci USA 1978;75:6107-9

Lee W, Samuel J, Zhang W, Rampal AL, Lachaal M, Jung CY. A myosin-derived peptide C109 binds to GLUT4-vesicles and inhibits the insulin-induced glucose transport stimulation and GLUT4 recruitment in rat adipocytes. Biochem Biophys Res Commun 1997;240:409-14

Nave BT, Haigh RJ, Hayward AC, Siddle K, Shepherd PR. Compartment-specific regulation of phosphoinositide 3-kinase by platelet-derived growth factor and insulin in 3T3-L1 adipocytes. Biochem J 1996;318 ( Pt 1):55-60

Neco P, Giner D, Viniegra S, Borges R, Villarroel A, Gutierrez LM. New roles of myosin II during vesicle transport and fusion in chromaffin cells. J Biol Chem 2004;279: 27450-7

Omata W, Shibata H, Li L, Takata K, Kojima I. Actin filaments play a critical role in insulin-induced exocytotic recruitment but not in endocytosis of GLUT4 in isolated rat adipocytes. Biochem J 2000;346 Pt 2:321-8

Park SY, Ryu J, Lee W. O-GlcNAc modification on IRS-1 and Akt2 by PUGNAc inhibits their phosphorylation and induces insulin resistance in rat primary adipocytes. Exp Mol Med 2005;37:220-9

Saitoh M, Ishikawa T, Matsushima S, Naka M, Hidaka H. Selective inhibition of catalytic activity of smooth muscle myosin light chain kinase. J Biol Chem 1987;262:7796-801

Sellers JR. Myosins: a diverse superfamily. Biochim Biophys Acta 2000;1496:3-22

Shechter Y. Trifluoperazine inhibits insulin action on glucose metabolism in fat cells without affecting inhibition of lipolysis.

Proc Natl Acad Sci U S A 1984;81:327-31

Steimle PA, Fulcher FK, Patel YM. A novel role for myosin II in insulin-stimulated glucose uptake in 3T3-L1 adipocytes. Biochem Biophys Res Commun 2005;331:1560-5

Tsien RY. New calcium indicators and buffers with high selectivity against magnesium and protons: design, synthesis, and properties of prototype structures. Biochemistry 1980;19:2396-404

Watson RT, Kanzaki M, Pessin JE. Regulated membrane trafficking of the insulin-responsive glucose transporter 4 in adipocytes. Endocr Rev 2004;25:177-204

Whitehead JP, Molero JC, Clark S, Martin S, Meneilly G, James DE. The role of $Ca^{2+}$ in insulin-stimulated glucose transport in 3T3-L1 cells. J Biol Chem 2001;276:27816-24

Worrall DS, Olefsky JM. The effects of intracellular calcium depletion on insulin signaling in 3T3-L1 adipocytes. Mol Endocrinol 2002;16:378-89

Yang C, Watson RT, Elmendorf JS, Sacks DB, Pessin JE. Calmodulin antagonists inhibit insulin-stimulated GLUT4 (glucose transporter 4) translocation by preventing the formation of phosphatidylinositol 3,4,5-trisphosphate in 3T3L1 adipocytes. Mol Endocrinol 2000;14:317-26.